ASTRONOMY & ASTROPHYSICS
SUPPLEMENT SERIES

Astron. Astrophys. Suppl. Ser. **132**, 13–20 (1998)

The kinematics of 867 galactic planetary nebulae⋆

S. Durand[1], **A. Acker**[1], **and A. Zijlstra**[2]

[1] UMR 7550, Équipe Évolution Galactique, Observatoire de Strasbourg, 11 rue de l'Université, F-67000 Strasbourg, France
[2] UMIST, department of Physics, P.O. Box 88, Manchester M60 1QD, UK

Received April 18, 1997; accepted March 24, 1998

Abstract. We present a compilation of radial velocities of 867 galactic planetary nebulae. Almost 900 new measurements are included. Previously published kinematical data are compared with the new high-resolution data to assess their accuracies. One of the largest samples in the literature shows evidence for a systematic velocity offset. We calculate weighted averages between all available data. Of the final values in the catalogue, 90% have accuracies better than 20 $\mathrm{km\,s^{-1}}$. We use this compilation to derive kinematical parameters of the galactic differential rotation obtained from least-square fitting and to establish the Disk rotation curve; we find no significal trend for the presence of an increasing external rotation curve. We examine also the rotation of the bulge; the derived curve is consistent with a linearly increasing rotation velocity with l: we find $V_{\mathrm{b,r}} = (9.9\pm1.3)l-(6.7\pm8.5)\,\mathrm{km\,s^{-1}}$. A possible steeper gradient in the innermost region is indicated.

Key words: catalogues — planetary nebulae — Galaxy (the): kinematics of

1. Introduction

Kinematical studies of the stellar populations in the inner parts of the Milky Way have mainly used RGB and AGB stars, observed in strategically chosen low-extinction windows (Morrison et al. 1990; Menzies 1990; Minniti 1994; Izumiura et al. 1995; Sevenster et al. 1997). These stars are both bright and numerous, and their metallicity covers a large range, allowing one to study the correlations between the kinematics and the chemical abundances in the Galaxy (Lewis & Freeman 1989; Ibata & Gilmore 1995). Recently, proper motions for some K giants have become available which provide the first striking signature of the bulge triaxiality (Zhao et al. 1994).

Planetary nebulae (hereafter PNe) trace a closely related stellar population which can also be used for such studies. They originate from intermediate and low initial-mass stars and therefore constitute a relatively old population. The optical spectrum of a PN is dominated by bright emission lines [recombination (H, He, a.o.) and collisionally excited ([OIII], a.o.) lines] allowing highly accurate radial velocity determinations. The observable life time is short, typically a few times 10^4 years. Therefore PNe are not very numerous in the Galaxy: the total population in the Galactic disk is estimated to be around 23 000 with an additional 2 000 in the bulge (Zijlstra & Pottasch 1991); older determinations range between 7 000 and 70 000 (see the compilation in Peimbert 1992) but with large dependencies on adopted distance scales. To date, about 1700 PNe are known in the Galaxy, classified in the Strasbourg-ESO Catalogue (Acker et al. 1992, hereafter SECAT) and its first supplement (Acker et al. 1996).

Although this suggests that PNe are useful tracers of Galactic kinematics, so far few papers have directly studied the kinematics of the PNe population. Schneider et al. (1983a; hereafter STPP83) made a compilation of all known PNe radial velocities at that time, correcting for systematic offsets between different sources. In a follow-up paper, Schneider & Terzian (1983b) derived a rising rotation curve in the outer Galaxy from 252 disk PNe. Kinman et al. (1988; hereafter KFL88) found evidence for bulge rotation from PNe radial velocities.

Since the compilation of STPP83, further radial velocity determinations of PNe have become available. Meatheringham et al. (1988; hereafter MWF88) presented radial and expansion velocities of 64 southern galactic planetary nebulae. In the same year KFL88 published radial velocities of 23 PNe (although with low accuracy), 15 of which were newly discovered. More recently, Kohoutek

Send offprint requests to: S. Durand

⋆ Table 2 is available in electronic form only, via anonymous ftp to cdsarc.u-strasbg.fr (130.79.128.5) or via http://cdsweb.u-strasbg.fr/Abstract.html

& Pauls (1995) presented well-determined radial velocities for 76 nebulae in the direction of the Galactic centre. Spyromilio (1995) gave accurate velocities for a few non-bulge PNe. Dopita & Hua (1997) measured radial velocities and fluxes of 52 southern PNe. Beaulieu (1996) made a deep and uniform narrow-band Hα imaging survey for PNe in the southern Galactic bulge; she measured radial velocities of 56 newly discovered PNe and also re-determined velocities for 317 previously known PNe. Finally, Zijlstra et al. (1997) presented high-accuracy velocities for 71 Galactic bulge PNe. There is significant overlap between these samples. Combined, there is now a larger and more accurate set of data available especially for the central regions of the Galaxy.

In this paper we present a new, up-to-date and homogeneous compilation of all PNe kinematical data known at the present time. A large number of new and previously unpublished measurements are included. The paper is presented as follows: Sect. 2 presents new radial velocities coming from our recent observations. In Sect. 3 the catalogue is presented, with a brief overview of its main characteristics. Finally, in Sect. 4, a preliminary study of the kinematics of the disk and the bulge is made.

2. New radial velocities

We have measured radial velocities of Galactic PNe in three separate observational programs. These concern 338 different PNe, 93 of which have for the first time a measured radial velocity. Some of these data have been published (Zijlstra et al. 1997); the remainder is presented here. The three programs are:

- **117 high-resolution data** (*ZASW*, in part published in Zijlstra et al. 1997).
  In the context of a study of expansion velocities of galactic bulge PNe and of PNe with [WC]-type nuclei, accurate radial velocities were measured for a sample of 119 PNe (this sample we will designate *ZASW*). The observations were carried out with the ESO 1.4 m CAT telescope with the short camera (CES), and performed in 1993 June, in 1993 July and in 1994 March. Two spectral ranges were selected, one around the [OIII] 5007 line (R = 30 000, 1993 June), the other including Hα and the [NII] red doublet (R = 60 000, 1993 July and 1994 March, see Acker 1993). Two PNe were discovered to belong to the Sagittarius Dwarf galaxy (Zijlstra & Walsh 1996), and therefore are excluded from our Galactic sample. The observations and the radial velocities of 71 bulge PNe (labelled as *(z)* in Table 2 (Col. 3) are presented in Zijlstra et al. 1997). The velocities of the 48 non-bulge PNe obtained from Hα and [NII] (R = 60 000) measurements are given in Table 2 Col. 3 (labelled as *(a)*).
- **130 medium-resolution data** (*ASC*).
  In the framework of chemical abundance determinations of galactic PNe high above the Galactic plane (Cuisinier et al. 1996), observations were conducted from 1993 to 1995 at the ESO 1.52 m telescope using the Boller & Chivens spectrograph and the 2048 $\times$ 2048 pixel FA27 CCD CCD. The wavelength range was 3600 $-$ 7400 Å with a spectral resolution $R \simeq 1500$. The entrance aperture was 1.5 $\times$ 3.4 arcsec.
- **247 low-resolution data** (*SA*).
  From 1983 to 1991, a spectrophotometric survey of galactic PNe was performed at the ESO 1.52 m telescope equipped with the Boller & Chivens spectrograph (see Acker et al. 1989b; Acker et al. 1992). Until 1987 the IDS detector was used, and afterwards a 512 $\times$ 1024 pixel CCD. The wavelength range was 3600 $-$ 7400 Å with a spectral resolution $R \simeq 800$. As the sample included a large number of Galactic bulge PNe, we measured the radial velocities of those 247 PNe despite the low resolution of the spectra.

The *ASC* and *SA* sample showed wavelength-dependent velocity residuals. To remove these, we applied a linear fit to these deviations per observing run (the slope of the fit changed between observing runs). The values on the blue part of the spectra appeared to be of poor quality (probably due to the low sensitivity of the detector) and were removed from the calculations. Each run was calibrated using the available *ZASW* values. Considering the mean dispersions of the spectra, measurements for which the uncertainties exceeded the expected ones were not included in the catalogue.

From the medium-resolution *ASC* data we obtained 130 radial velocities of sufficient quality, with a mean uncertainty of about 20 km s^{-1}. From the *SA* data we obtained 247 acceptable measurements with a mean uncertainty of about 40 km s^{-1}.

The galactic distribution of these 494 new data (including data published in Zijlstra et al. 1997) is displayed in Fig. 1.

3. The catalogue

The catalogue contains:

- 494 new high-, medium- and low-resolution measurements described in Sect. 2.
- 373 nebulae from Beaulieu (1996), 73 from Kohoutek & Pauls (1995), 52 from Dopita & Hua (1997), 3 from Spyromilio (1995) and 5 from Kraan-Korteweg et al. (1996).
- 577 radial velocities published in the SECAT (including STPP83, MWF88 and KFL88 data).

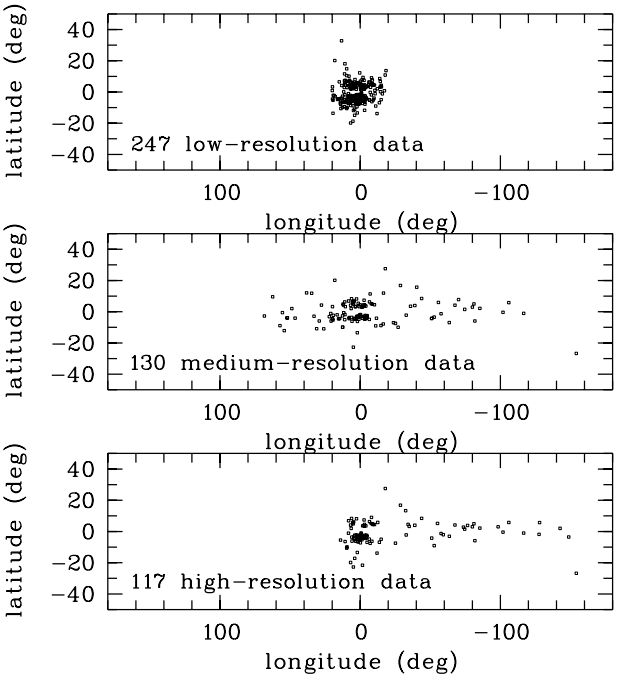

Fig. 1. Galactic positions of the new 494 radial velocities – top: 247 *SA* data; – middle: 130 *ASC* data; – bottom: 117 *ZASW* data

3.1. Uncertainties and systematic deviations of literature data

The literature data originates mostly from a number of individual surveys. In order to test the accuracies of these surveys, we compare the lists with the high-resolution *ZASW* data, for those objects in common.

Figure 2 (right) displays the comparison of the literature data data with the high-resolution *ZASW* data for several surveys. Two individual objects of Dopita & Hua, He 2 − 118 and He 2 − 97, show a very large discrepancy with the *ZASW* values (see Fig. 2, right) and are excluded in the statistics of Table 1. Both have late-type [WC] central stars, and in such objects a velocity shift is sometimes seen between nebular and stellar lines (e.g. Menzies & Wolstencroft 1990; Le Bertre et al. 1989). Two large surveys included in STPP83 (Minkowski 1957 (right panel) and Mayall 1964 (left panel)) show significant scatter. Both are published only as private communications in the catalogue of Perek & Kohoutek (1967) and may originate from a variety of separate measurements.

Table 1 presents the systematic deviations and the scatter for the principal sources. We calculate the significance of the systematic offsets between the samples by applying student's t statistics on the objects in common between *ZASW* and the individual samples. An uncertainty of 2 $\mathrm{km\,s^{-1}}$ is assigned to *ZASW* (Zijlstra et al. 1997). The resulting probabilities are listed in Table 1. The offset is taken to be significant if the probability is less than 0.01. This is the case only for Minkowski (1957). STPP83 added 4 $\mathrm{km\,s^{-1}}$ to all Webster and Kalnajs (1982) velocities based on a comparison with 10 previous measurements. This correction is not confirmed at the required significance level.

Table 1. Systematic deviations of the principal sources of available data compared with the *ZASW* data (n is the number of compared PNe) (offsets stand for $< V_{\mathrm{ZASW}} - V_i >$). The probability gives the likelihood that the offset is due to chance, using student's t statistics

Sources	offsets	disp.	n	prob.
AS (1992)	−4.1	39.3	52	0.46
ASC (1995)	−2.7	18.4	55	0.29
Campbell & Moore (1918)	−3.0	4.4	11	0.058
Minkowski (1957)	−16.3	15.0	39	$4.8\,10^{-8}$
Mayall (1964)	−3.0	42.4	23	0.74
Acker (1975)	−6.4	9.6	08	0.1
Webster & Kalnajs (1982)	−2.7	2.9	11	0.02
Kohoutek & Pauls (1995)	+0.8	4.2	07	0.66
Dopita & Hua (1997)	+4.3	8.3	10	0.14
Beaulieu (1996)	+4.1	15.2	50	0.064

The data from Mayall (1964) shows a large scatter which is well approximated by a 1-σ uncertainty of 40 km $\mathrm{s^{-1}}$ (Table 1). This is much larger than the 25 km $\mathrm{s^{-1}}$ assigned by STPP83. After removing the systematic offset for the Minkowski (1957) data, an uncertainty of 15 km $\mathrm{s^{-1}}$ remains (as compared to 11 km $\mathrm{s^{-1}}$ assigned in STPP83). The lists by MWF88 and KFL88 are not included in Table 1 as only a few of their objects are common with *ZASW* data. We assign an estimated uncertainty of 15 km $\mathrm{s^{-1}}$ for all KFL88's velocities, based on the resolution of their spectra which is similar to Beaulieu's data. KFL suggest themselves an uncertainty of 8 km $\mathrm{s^{-1}}$.

3.2. The catalogue

Following the discussion above, we correct the sample of Minkowski (1957) for a systematic offset of -16.3 $\mathrm{km\,s^{-1}}$. The offsets for other samples are not considered significant. For each PN the average value of its radial velocity is now obtained by weighting each existing velocity by the inverse of the square of its associated error, thus giving low weight to the poorest data:

$$\bar{V} = \left[\sum_i \bar{V}_i / Err_i^2\right] \Big/ \left[\sum_i 1/Err_i^2\right]. \quad (1)$$

For the mean total error, we choose as the best estimate the larger of the two quantities:

$$Err = \left[\sum_i 1/Err_i^2\right]^{-\frac{1}{2}} \quad (2)$$

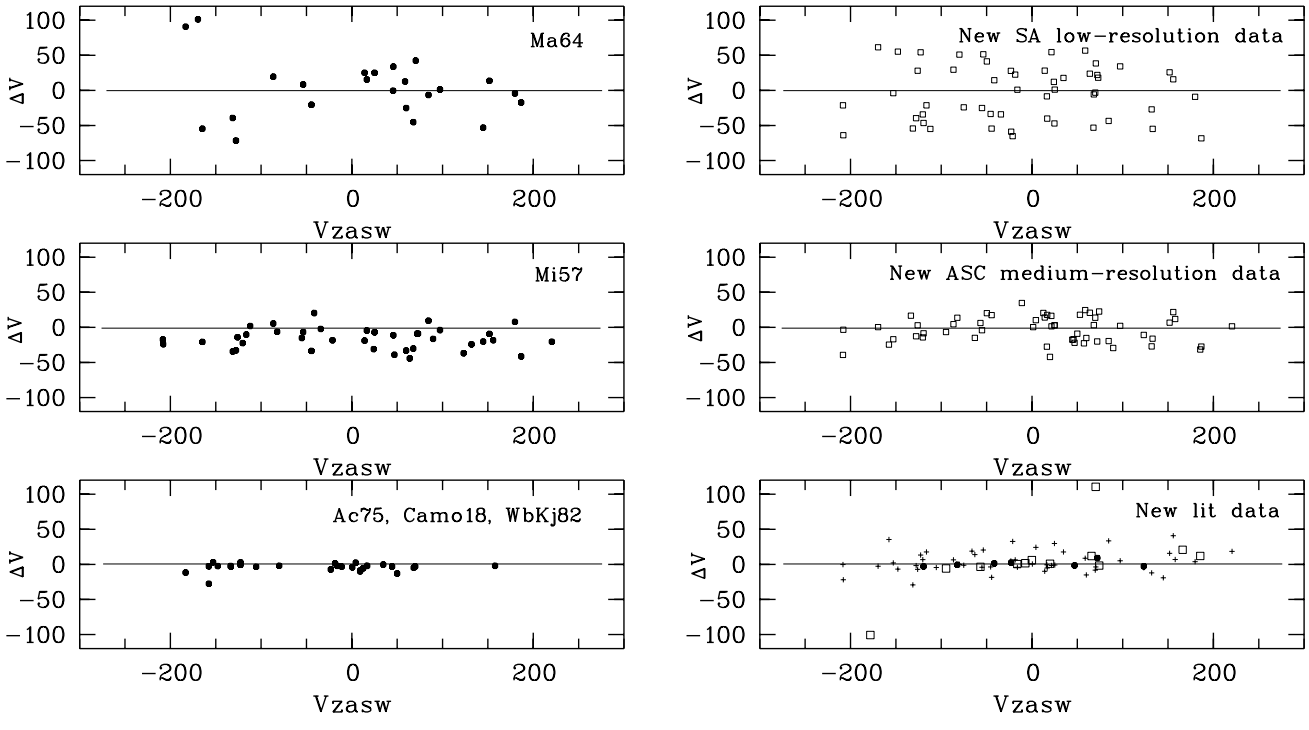

Fig. 2. Left: Comparison of the five principal sources of STPP83 with the high-dispersion *ZASW* data (ΔV stands for $(V_{\rm ZASW} - V_i)$); the literature data are globally overestimated and present various uncertainties depending from their authors. Right: Comparison of recent data with the *ZASW* data (ΔV stands for $(V_{\rm ZASW} - V_i)$); in New lit data: open squares are DH97, crosses are SB96 and circles are KP95 data

and

$$Err_{\rm rel}=\left[\sum_i(\bar{V}_i-\bar{V})/Err_i^2\right]\Big/\left[(P-1)\sum_i 1/Err_i^2\right]^{\frac{1}{2}}. \quad (3)$$

The catalogue is presented in Table 2 as follows:
Column 1: the standard PNG numbers as adopted in the SECAT.
Column 2: usual name of the PN.
Column 3: new high-resolution ZASW velocities.
Column 4: new medium-resolution ASC velocities.
Column 5: new low-resolution SA velocities.
Column 6: literature data published after 1992 with references.
Column 7: literature data from the SECAT (some are corrected from offsets seen in Table 1) with references.
Column 8: adopted radial velocities with their uncertainties.

4. A kinematical overview of the catalogue

4.1. Galactic distribution

Figure 3 (top) displays the 867 radial velocities versus galactic longitude; most PNe are located in the direction of the galactic Centre and characterized by highly elongated orbits. According to their galactic positions (see middle panel of Fig. 3), most PNe are concentrated towards the galactic disk, and a few PNe may belong to a halo population. Only BoBn 1, a very old and metal-deficient halo star (108.4−76.1, see top of Fig. 3) exhibits a completely atypical motion. Additional measurements of its velocity (the only one available was made in 1977 by Boesharr & Bond) would be desirable in order to definitively confirm this value.

Figure 3 (bottom) displays the distribution in longitude of the 867 PNe according to their velocity uncertainties: about 90% of the sample have velocity errors better than 20 km s^{-1}. The largest uncertainties tend to be found among the bulge PNe.

The extrema of the radial velocities towards the galactic Centre have decreased since STPP83 paper: for example, the value of 241.0 ± 11.0 km s^{-1} of M1−37 (2.6 − 3.4) in STPP83 now becomes 220.5 ± 0.9 km s^{-1}, and that of M4−6 (358.6 + 1.8) has gone from -292.0 ± 11.0 km s^{-1} to -268.1 ± 5.5 km s^{-1}.

4.2. The kinematics of disk PNe

The use of PNe for establishing the Disk rotation curve is hampered by the large uncertainty of the distances.

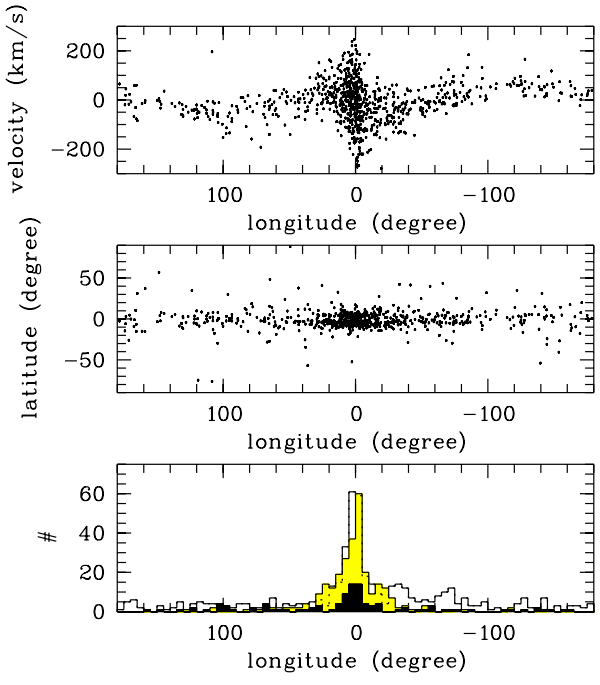

Fig. 3. Top: heliocentric radial velocities of the 867 PNe versus their galactic longitude. Middle: galactic positions of the 867 PNe of the present catalogue. Bottom: distribution in longitude of the 867 PNe according to their velocity uncertainties. White represents an error of < 10 km s^{-1} (482 PNe), grey $10 \leq$ error < 20 km s^{-1} (281 PNe), and black an error of ≥ 20 km s^{-1} (104 PNe)

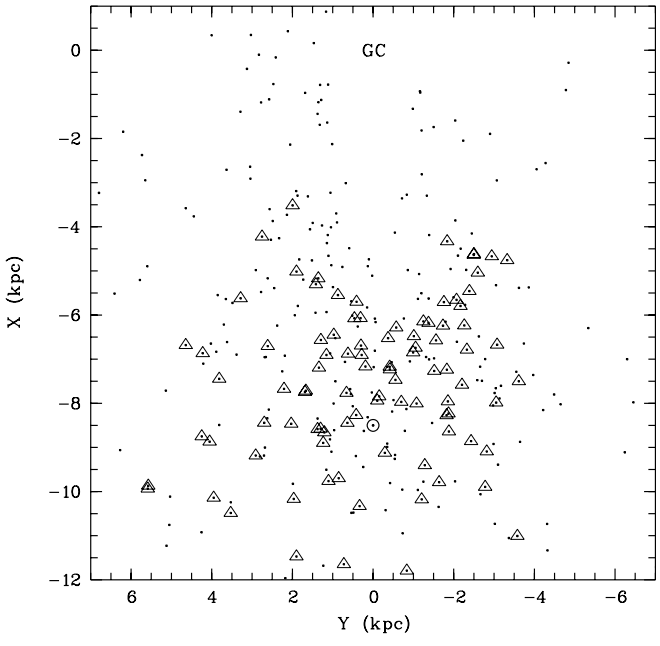

Fig. 4. Galactic distribution of the 96 disk PNe projected on the XY plane; the positions of the sun (−8.5,0) and of the galactic center (0,0) are indicated

In our study we use the statistical distance scale of Zhang (1995), which is an average of two distance scales: one is based on the correlation between the ionized mass and the radius, the other on the correlation between the radio continuum surface-brightness temperature and the nebular radius. The intrinsic uncertainty in this scale (not counting possible systematic effects) is not known but is likely to be in excess of 30% (1 sigma) for each object, from comparison with van de Steene & Zijlstra (1994, 1995). These large uncertainties will tend to smooth out structure in the rotation curve and may also introduce systematic effects (Zijlstra & Pottasch 1991).

We selected from our sample 100 PNe located at $|l| > 7°$ (in order to avoid contamination by bulge objects) and < 200 pc above the galactic plane (in order to select objects with near-circular orbits). 4 PNe with residual velocities larger than 100 km s^{-1} were considered interlopers and removed from the sample. Figure 4 displays the galactic distribution of the 96 PNe projected onto the galactic plane (triangles) superimposed on all other PNe with estimated distances in the same region. Our sample seems to abruptly end at $R_{\rm gc} = 5$ kpc which could be due to a local spiral arm (see for instance Georgelin & Georgelin 1976, for a description of the galactic spiral structure from HII regions data). Extinction by dusty molecular clouds in such an arm could hide farther PNe from sight.

4.2.1. The local galactic rotation

Consider a star on a purely circular orbit at galactocentric radius R: its heliocentric radial velocity can be expressed by the well-known formula:

$$\begin{aligned} V_{\rm r}^{\rm mod} &= -u_\odot \cos l \cos b - v_\odot \sin l \cos b - w_\odot \sin b \\ &- 2\,A\,(R - R_\odot) \sin l \cos b \\ &+ (\frac{A_2}{2}\,(R - R_\odot)^2) \sin l \cos b \\ &+ K \end{aligned} \quad (4)$$

where:

- $u_\odot$, $v_\odot$ and $w_\odot$ are the components of the solar motion with respect to the local standard of rest, respectively in the radial, azimuthal and vertical directions ($u_\odot$ is taken to be positive toward the galactic center). As our stellar sample is restricted to low vertical heights we will not be able to constrain $w_\odot$; instead we fix its value to the standard one (7.3 km s^{-1}).
- The second row of the equation expresses the differential galactic rotation to first order; A is the Oort constant.
- In the third row A_2 is the second order coefficient of the derivative of the rotation speed with respect to R. This expansion to second order in $(R - R_\odot)$ allows us to use the kinematics of stars located further from the Sun.

Table 3. Kinematical parameters obtained from least-square fitting of Eq. (4)

$u_\odot$	16.0 ± 4.8 ($\mathrm{km\,s^{-1}}$)
$v_\odot$	24.8 ± 3.8 ($\mathrm{km\,s^{-1}}$)
$R_\odot$	8.7 ± 2.1 (kpc)
A	14.4 ± 1.7 ($\mathrm{km\,s^{-1}\ kpc^{-1}}$)
A_2	13.0 ± 0.9 ($\mathrm{km\,s^{-1}\ kpc^{-2}}$)
K	5.1 ± 2.8 ($\mathrm{km\,s^{-1}}$)

– The last row gives the expression of the K-term of local galactic expansion.

We fit the above formula by minimizing:

$$\chi^2 = \sqrt{\sum_{i=1}^{N} (\frac{v_\mathrm{r}^{\mathrm{obs}_i} - v_\mathrm{r}^{\mathrm{mod}_i}}{\Delta\, v_\mathrm{r}^i})^2} \quad (5)$$

with N the total number of stars in the sample and $\Delta\, v_\mathrm{r}^i$ the uncertainty assigned to the radial velocity of the i^{th} star.

Table 3 presents results obtained from a straightforward least-square fitting of Eq. (4).
We apply our fitting procedure by testing also various cases, as for example the non-inclusion of the A_2 term: it seems necessary to include it in the fitting procedure since without it the fits converge to unphysical values. The value of the A_2 term is largest than for other determinations (see for example Pont et al. 1994, using Cepheids data); this could be explained by the great uncertainties on PNe distances.

$u_\odot$ and $v_\odot$ appear different from the "standard" values (which are equal to 10.4 and 14.8 $\mathrm{km\,s^{-1}}$ respectively). A high value of $v_\odot$ is usually associated with evolved populations: it is related to the asymmetric drift which becomes more important with late-type stars (see Fig. 6 in Jahreiss & Wielen). The mean value of the asymmetric drift of our 96 PNe sample is about 10 $\mathrm{km\,s^{-1}}$ in our model, but with low confidence. The high value of the $u_\odot$ parameter may point to the existence of an *outward* motion of the local standard of rest as already proposed for example by Blitz & Spergel (1991).

The value of the K-term is consistent with zero given the uncertainties inherent in a multi-parameter fit. A non-zero value would be related to imperfections in the data (e.g. a systematic velocity offset or a bias) or imperfections in the rotation curve (e.g. the existence of residual non-axisymmetrical motions). Given the uncertainty, there is no conclusive evidence for a non-zero value.

4.2.2. The disk rotation curve

In order to test the galactic rotation curve as function of galactocentric distance of PNe, we first calculate the PNe galactic-standard-of-rest velocities using the formula:

$$V_\mathrm{rot} = \left(\Theta_\odot + \frac{V_\mathrm{lsr}}{\sin\, l\, \cos\, b}\right) \frac{R_\mathrm{p}}{R_\odot} \quad (6)$$

where V_lsr is calculated from the above galactic rotation model, and $\Theta_\odot = R_\odot\,(A - B) = 8.7\,(14.4 + 12.4) = 233$ km s^{-1}.

In Fig. 5 we display the galactic distribution of the 96 disk PNe and the rotation velocities versus Galactocentric distance. The distance is normalized to the Solar galactocentric distance $R_\odot = 8.7$ kpc. In the bottom panel of the same figure we display the binned galactic rotation curve as provided by our PNe sample. Some authors (Amaral et al. 1996; Maciel & Dutra 1992) have found evidence for large-scale features in their rotation curve, in particular a broad maximum near $R = 6$ kpc (corresponding here to $R/R_\odot = 0.75$) and a local decrease. Despite the insufficient number of objects and the (likely) smoothing due to the uncertainties in the individual distances, our curve recovers the same behaviour, but with a lower amplitude. Those features have also been detected in CO and HI data (Clemens 1985). There is also a slight indication of lower velocities around 11 kpc.

The 2 isolated points located at $R_\mathrm{gc} = 12.05$ and 12.65 kpc may give the appearance of an increasing outer rotation curve, but their presence cannot be in any way conclusive.

4.3. The rotation of the bulge

Various tracer populations have been used to constrain the structure and kinematics of the galactic bulge (Frogel et al. 1990; Minniti et al. 1992; Whitelock & Catchpole 1992; Beaulieu 1996). These studies gave rather similar results (see also a brief review in Menzies 1990): the rotation curve increases quasi-linearly with l, with a mean slope of about $10 - 15$ $\mathrm{km\,s^{-1}\,l^{-1}}$ but possibly somewhat steeper near the center. Velocity dispersions are typically $70 - 120$ $\mathrm{km\,s^{-1}}$. A general trend is shown for the metal-rich populations to rotate a little faster than metal-poor ones; the velocity dispersion of the stars tends to decrease away from the Galactic Center.

KFL88 analysed a sample of 147 PNe ranged between $|l| < 10$ and $|b| < 5.5$ and found indications for the rotation of the bulge: they fitted a linear equation in (l, V_c) and found the relation $V_\mathrm{c} = (12.0 \pm 1.9)l - (13.6 \pm 8.6)\,\mathrm{km\,s^{-1}}$. They point out that due to projection effects the observed slope should be considered as lower limit.

To compare with Kinman et al. (1988), we relax our selection criteria for bulge membership: $|l| < 10.0$ degree and $|b| < 7.0$ degree; rejecting PNe with optical angular diameter > 20 arcsec and/or radio flux $F_{6\,\mathrm{cm}} > 100$ mJy (e.g. Acker & Pottasch 1989a). This sample contains 279

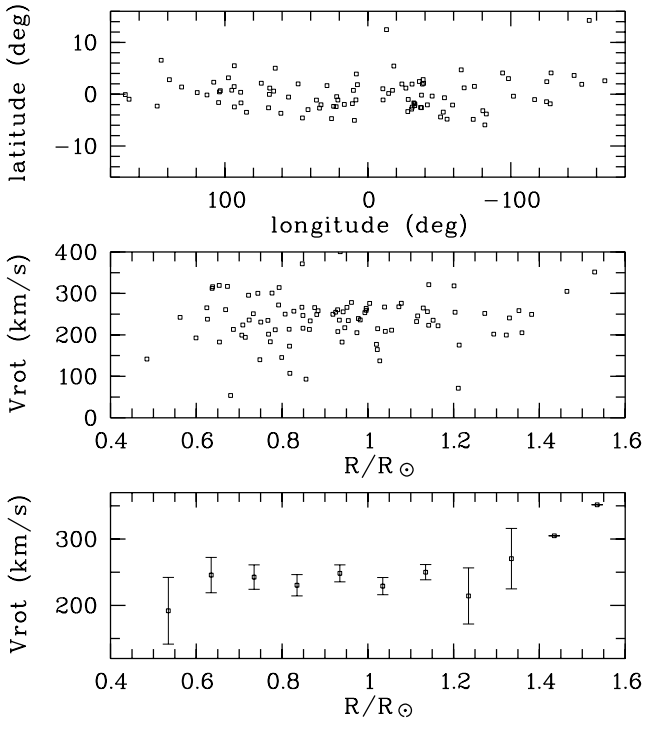

Fig. 5. Top: galactic distribution of the 96 disk PNe at $|z| < 200$ pc. Middle: galactic longitude versus rotation velocity. Bottom: bin and linear fit of the middle graph. The data are averaged in 0.1 bins. The error bars include only the standard error of the mean in each bin

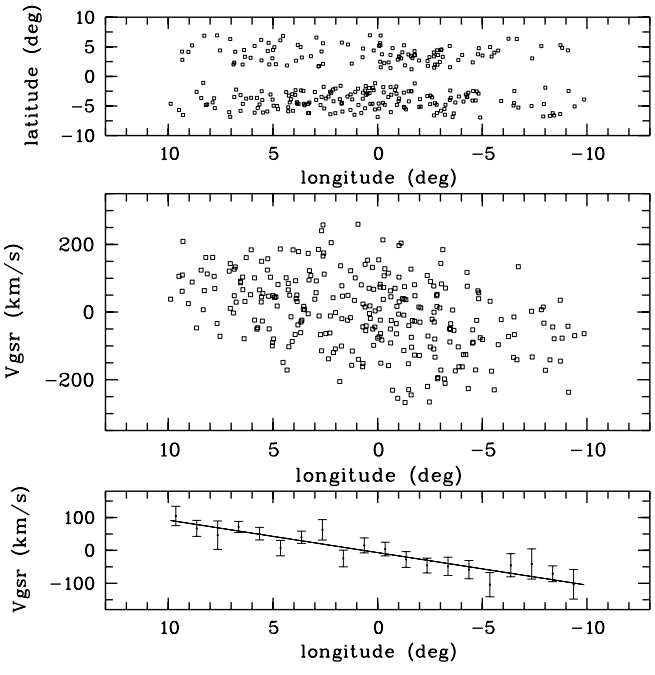

Fig. 6. Top: galactic distribution of 279 bulge PNe. The effects of the absorption in the galactic plane are evident. Middle: galactic longitude versus galactocentric velocity. Bottom: bin and linear fit of the middle graph. The data are averaged in bins of one degree of longitude. The error bars include only the standard error of the mean in each bin

PNe. Figure 6 displays the galactic distribution of this PNe sample; the incompleteness is evident in the galactic plane (top panel). The middle panel shows the galactic-standard-of-rest velocities versus the longitude, and the bottom panel shows the same data in one-degree bins, with error bars representing only standard errors of the mean. The linear fit shown in the bottom of Fig. 6 has a slope of (9.9 ± 1.3) km s^{-1}. The zero longitude offset is -6.7 km s^{-1}. All these results are in good agreement with KFL88.

Table 5 compares values for the bulge rotation derived from different samples. The first three lines show the results from the restricted criterion for bulge membership, using different limits for the Galactocentric distances and only velocities better than 20 km s^{-1}. The fourth line shows the result from the relaxed criterion mentioned above. In all cases there is good evidence for the rotation of the bulge. The gradient b may increase very close to the Centre but the uncertainties are much larger for this smaller samples. Interestingly, the relaxed sample gives essentially the same result. The offset at zero longitude (a) is within the uncertainties zero.

The last rows of Table 5 shows for comparison previous determinations. The values are in general consistent, although the location of the tracer populations are not identical. The planetary nebulae probably provide the best coverage close to the Centre, whereas the AGB stars give better coverage at high latitudes.

5. Conclusion

We have presented in this paper an up-to-date compilation of all known galactic PNe radial velocities. After averaging all available data, 90% of the kinematics data of the 867 PNe of the catalogue have accuracies better than 20 km s^{-1}. We evaluated the kinematical parameters of the PNe differential galactic rotation by a least-square method and established the rotation curve of the Galaxy for $3.2 < R < 12.8$ kpc. We found no significal trend for an increasing in the external rotation curve. The rotation of the bulge is found to be (9.9 ± 1.3) km s^{-1} deg^{-1}.

Acknowledgements. We are deeply indebted to Bjorn Stenholm for his participation in some of the observations. It's a great pleasure to thank Sylvie Beaulieu for generously providing us her bulge velocities before their publication. We also thank François Cuisinier for making some of his data available to us.

Table 5. bulge rotation fitted by $a + bl$ km s^{-1}

Sample of PNe	Number of stars	a (km s^{-1})	b (km s^{-1} deg^{-1})	σ (km s^{-1})
$D_{gc} < 3$ kpc	87	-9.7 ± 11.7	10.2 ± 2.0	108 ± 12
$D_{gc} < 2$ kpc	60	-18.5 ± 14.6	12.2 ± 3.3	113 ± 15
$D_{gc} < 1$ kpc	22	9.4 ± 27.5	32.5 ± 12.0	129 ± 28
full sample	279	-6.7 ± 8.5	9.9 ± 1.3	100
Other populations:				
K-giants ($(l, b) = (8°,7°)$) (Ref. 1)	196		8.3 ± 0.6	71.9 ± 3.6
SiO stars ($b = 7°$) (Ref. 2)	134	-17.7 ± 7.6	10.8 ± 1.2	82.4
Miras ($\|l\| < 5°$) (Ref. 3)	25	7.4 ± 18	22.6 ± 8	90.5 ± 13
Miras ($\|l\| < 15°$, $7° < \|b\| < 8°$) (Ref. 4)	26	-8.2 ± 15.7	9.8 ± 1.9	76 ± 11

Ref. 1: Minniti 1996; 2: Izumiura et al. 1995; 3: Catchpole 1990; 4: Menzies 1990.

References

Acker A., 1975, A&A 40, 415
Acker A., Pottasch S.R., 1989a, A&A 221, 123
Acker A., Jasniewicz G., Köppen J., Stenholm B., 1989b, A&AS 80, 201
Acker A., Ochsenbein F., Stenholm B., Tylenda R., Marcout J., Schon C., 1992, Strasbourg-ESO catalogue of galactic planetary nebulae, ESO (**SECAT**)
Acker A., Marcout J., Ochsenbein F., et al., 1996, First Supplement to the Strasbourg-ESO catalogue of Galactic Planetary Nebulae, published by the Observatoire de Strasbourg
Amaral L., Ortiz R., Lépine J., Maciel W., 1996, MNRAS 281, 347
Beaulieu S., 1996, Thesis, Australian National University
Blitz L., Spergel D., 1991, ApJ 370, 205
Boeshaar G., Bond H., 1977, ApJ 213, 421
Campbell W.W., Moore J.H., 1918, Publ. Lick Observatory 13, 75
Catchpole M., 1990, ESO/CTIO Workshop on Bulges of Galaxies, p. 111
Clemens D., 1985, ApJ 295, 422
Cuisinier F., Acker A., Köppen J., 1996, A&A 307, 215
Dopita M.A., Hua C.T., 1997, ApJS 108, 515
Frogel J., Terndrup D., Blanco V., Whitford A., 1990, ApJ 353, 494
Georgelin Y., Georgelin P., 1976, A&A 49, 57
Honma M., Sofue Y., 1996, PASJ 48, 103
Ibata R., Gilmore G., 1995, MNRAS 275, 605
Izumiura H., Deguchi S., Hashimoto O., et al., 1995, ApJ 453, 837
Jahreiss H., Wielen R., 1983, in the IAU Coll. 76 Nearby stars and stellar luminosity functions, p. 277
Kinman T.D., Feast M.W., Lasker B.M., 1988, AJ 95, 804 (**KFL88**)
Kohoutek L., Pauls R., 1995, A&AS 111, 493
Kraan-Korteweg R., Fairall A., Woudt P., van de Steene G.C., 1996, A&A 315, 549
Lewis J., Freeman K., 1989, AJ 97, 139
Le Bertre T., Epchtein N., Gouiffes C., Heydari-Malayeri M., Perrier C., 1989, A&A 225, 417
Maciel W., Dutra C., 1992, A&A 262, 271
Mayall N.U., 1964 (priv. comm. in: Perek & Kohoutek 1967)
Meatheringham S., Wood P., Faulkner D., 1988, ApJ 334, 862 (**MWF88**)
Menzies J., 1990, ESO/CTIO Workshop on Bulges of Galaxies, p. 115
Menzies J.W., Wolstencroft R.D., 1990, MNRAS 247, 177
Minkowski D.K., 1957 (priv. comm. in: Perek & Kohoutek 1967)
Minniti D., White S., Olszewski E., Hill J., 1992, ApJ 393, L47
Minniti D., 1994, PASP 106, 813
Minniti D., 1996, ApJ 459, 579
Morrison H., Flynn C., Freeman K., 1990, AJ 100 (4), 1191
Peimbert M., 1992, in: Planetary Nebulae, IAU Symp. 180, Weinberger R. and Acker A. (eds.). Kluwer, Dordrecht, p. 523
Perek L., Kohoutek L., 1967, catalogue of galactic planetary nebulae, Czechoslovak Institute of Science, Prague
Pont F., Mayor M., Burki G., 1994, A&A 285, 415
Schneider S.E., Terzian Y., Purgathofer A., Perinotto M., 1983a, ApJS 52, 399 (**STPP83**)
Schneider S.E., Terzian Y., 1983b, ApJ 274, L61
Sevenster M.N., Chapman J.M., Habing H.J., Killeen N.E.B., Lindquist M., 1997, A&AS 122, 79
Spyromilio J., 1995, MNRAS 277, L59
van de Steene G.C., Zijlstra A.A., 1994, A&AS 108, 485
van de Steene G.C., Zijlstra A.A., 1995, A&A 293, 541
Webster B.L., Kalnajs A., 1982 (priv. comm. in Schneider et al. 1983a)
Whitelock P., Catchpole R., 1992, in: The center, Bulge, and Disk of the Milky Way, L. Blitz (ed.). Kluwer Academic Publishers, p. 103
Zhang C., 1995, ApJS 98, 659
Zhao H., Spergel D., Rich M., 1994, AJ 108, 2154
Zijlstra A.A., Pottasch S.R., 1991, A&A 243, 478
Zijlstra A.A., Walsh J., 1996, A&A 312, L21
Zijlstra A.A., Acker A., Walsh J., 1997, A&AS 125, 289